
Surface diffusion of carbon atoms as a driver of interstellar organic chemistry

In the format provided by the authors and unedited

Supplementary Information

Surface Diffusion of Carbon Atoms as a Driver of Interstellar Organic Chemistry

Masashi Tsuge^{1*}, Germán Molpeceres², Yuri Aikawa², and Naoki Watanabe¹

¹Institute of Low Temperature Science, Hokkaido University, Sapporo 060-0819, Japan.

² Department of Astronomy, Graduate School of Science, The University of Tokyo, Tokyo 113-0033, Japan

*e-mail: tsuge@lowtem.hokudai.ac.jp

S1. Fraction of physisorbed (weakly bound) C atoms on ASW

As shown in Supplementary Fig. 3, the PSD-REMPI signal for C atoms during continuous deposition at 10 K increased linearly in the early stage ($t < 1,000$ s) and began saturating after 1,000–1,500 s of deposition, corresponding to a C-atom fluence of $(1-1.5) \times 10^{13}$ atoms cm^{-2} , indicating the presence of loss processes. The early stage was fitted by a linear function, represented by the red line in Supplementary Fig. 4. The vertical axis was scaled such that the saturation value was unity. In this figure, the vertical gap between the black squares and the red line corresponds to the number of C atoms lost during deposition. For example, at a C-atom fluence of 2×10^{13} atoms cm^{-2} , approximately 30% loss was observed. However, assuming an adsorption site density of 1×10^{15} sites cm^{-2} for the np-ASW sample, the coverage was ~ 0.02 at this stage. Because C atoms should be incapable of diffusing long distances at 10 K, the C atom loss due to the recombination reaction $\text{C} + \text{C} \rightarrow \text{C}_2$ is negligible at this low coverage. Other possible processes include the formation of H_2CO and change from a physisorbed to a chemisorbed state. From the PSD-REMPI experiments for detecting H_2CO , we confirmed that the formation of H_2CO was not responsible for the loss, i.e., no increase in H_2CO was observed during C-atom decay. Therefore, PSD-REMPI method can only detect physisorbed C atoms (that is, C atoms trapped in relatively shallow binding sites), and that some of the physisorbed C atoms will be chemisorbed during deposition.

The PSD-REMPI intensities decayed even at 10 K after the termination of C atom deposition (Supplementary Fig. 5a). The attenuation curves were fitted using a single exponential function:

$$[\text{C}]/[\text{C}]_0 = (1 - b) \exp(-k_{\text{loss}}t) + b, \quad (\text{S1})$$

where b is the asymptotic value representing the number of detectable C atoms remaining for a long time. In the temperature range of 10–30 K, the rate constant k_{loss} was found to be almost temperature independent, as shown in Supplementary Fig. 5b. Temperature independence indicates that the loss process is dominated by an over-the-barrier process with an extremely low barrier or is promoted by nonthermal mechanisms, such as quantum mechanical tunneling. In the former case, the deposited C atoms should be readily chemisorbed and cannot be detected using the PSD-REMPI method, which is inconsistent with the observations. Moreover, assuming the low barrier (for example, 100 K), to obtain $1/k_{\text{loss}} \sim 1,100$ s at the temperature of 10 K (shown in Supplementary Fig. 5a and 5b), a frequency factor $<10^2$ s $^{-1}$ must be assumed in the Arrhenius equation, which is significantly smaller than the typical value of 10^{12} s $^{-1}$, indicating that the scenario for over-the-barrier process does not work. Therefore, we propose that the loss process (that is, transformation from physisorbed to chemisorbed states) must occur strictly via nonthermal mechanisms, such as quantum mechanical tunneling. The migration from physisorbed to chemisorbed state by the quantum mechanical tunneling has been treated based on Bell's formula; see Thi et al. (2020)¹ for details.

Similar measurements and analyses were performed by varying the fluence of C atoms from 1.5×10^{12} to 2.5×10^{13} atoms cm $^{-2}$ with the sample temperature of 10 K. The asymptotic values are plotted as a function of the C-atom fluence in Supplementary Fig. 6. The asymptotic values decreased as a function of the C-atom fluence and became constant at 0.1 for fluences greater than 1×10^{13} atoms cm $^{-2}$, which corresponds to the fluence at which the PSD-REMPI signal began saturating (see Supplementary Fig. 1). To extrapolate the observed trend to the low-fluence limit, the observed data were fitted to a single exponential function with an offset (red line). According to this analysis, the b value approaches 0.4 when the C-atom fluence is significantly small. As mentioned in the main text, 30% of the deposited C atoms are readily consumed during H₂CO formation;² therefore, at a low C-atom fluence relevant to realistic astronomical conditions, approximately 30% of the deposited C atoms are considered to remain physisorbed (70% \times 40%).

The binding sites are divided into three types: (i) C atoms readily react to produce H₂CO, (ii) C atoms remain physisorbed within the laboratory time scale, and (iii) initially physisorbed C atoms are slowly chemisorbed (see Supplementary Fig. 7 for potential energy schemes for types ii and iii). The experimental results (presented in Supplementary Fig. 6) can be rationalized if the number of type-ii sites is small, and these sites are preferentially occupied at low coverage. In particular, if the deposited C-atoms are equally

distributed to each type of site, the experimental results cannot be explained, and “adsorption dynamics” play an important role.

Because the translational energy of the C atoms colliding with the np-ASW sample is considerably high ($>2,000$ K), it can affect the adsorption dynamics. Additional experiments were performed to verify this hypothesis. In these experiments, C atoms and neon, with a ratio 1:2,000, were co-deposited over np-ASW maintained at 6 K. After deposition, the sample was warmed to 15 K to sublimate the neon matrix and immediately cooled to 10 K to observe the behavior of the PSD-REMPI signal. Using this procedure, very cold C atoms (10–15 K) were deposited on the np-ASW. From the decay curves of the PSD-REMPI signals, we determined b values for C-atom fluences of 0.5, 1.0, 2.0, and 2.5×10^{13} atoms cm^{-2} (Supplementary Fig. 8). The b values determined for the co-deposition experiments (red circles) were similar to those obtained for the simple C-atom deposition experiments (black squares), indicating that the translational energy of the C atoms was unrelated to the adsorption dynamics. In particular, the translational energy was readily dissipated by the surface of the np-ASW.

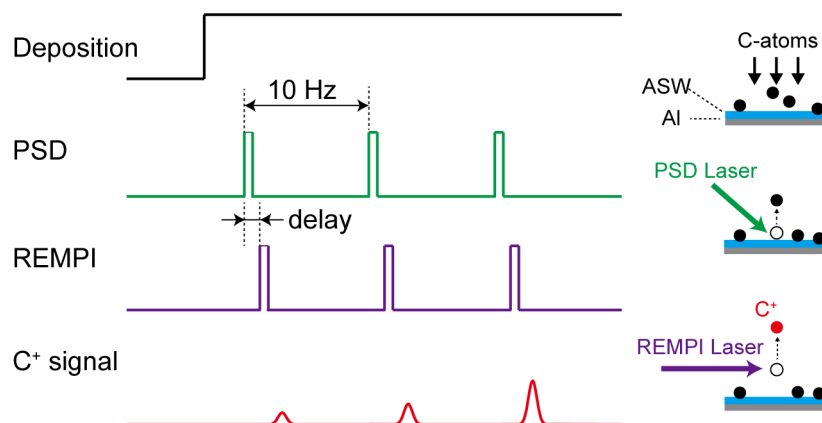
The asymptotic value b was determined for temperatures of 20 and 25 K with various C-atom fluences, as shown in Supplementary Fig. 9. At 20 K, the obtained b values show a trend similar to that at 10 K, with a low fluence limit of ~ 0.25 . At 25 K, b values were mostly constant at approximately 0.05. When comparing the b values at a given fluence, they decreased as a function of temperature. This trend indicates that the transformation from a physisorbed state to a chemisorbed state by quantum mechanical tunneling is thermally activated.

References

1. Thi W. F., Hocuk S., Kamp I., Woitke P., Rab Ch., Cazaux S, Caselli, P. Warm Dust Surface Chemistry: H₂ and HD Formation. *Astron. Astrophys.*, **634**, A42 (2020).
2. Molpeceres G., Kästner J., Fedoseev G., Qasim D., Schömig R., Linnartz H., et al. Carbon Atom Reactivity with Amorphous Solid Water: H₂O-Catalyzed Formation of H₂CO. *J. Phys. Chem. Lett.*, **12**, 10854–10860 (2021).

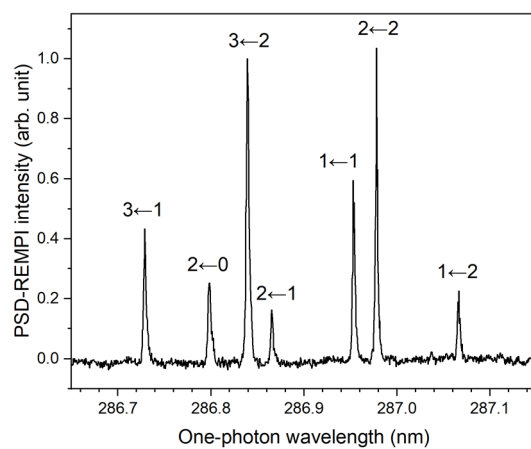
Supplementary Table 1 | Activation energies derived in this work and assumed in the literature.

Reference	E_{sd} (K)	Note
Hasegawa & Herbst (1993)	280	Calculated according to $E_{sd}/E_{des} = 0.35$ with $E_{des} = 800$ K
This work	1,020	Determined by experiments
See note	3,500	Calculated according to $E_{des} = 10,000$ K (Wakelam et al. 2017) and $E_{sd}/E_{des} = 0.35$ (Garrod et al. 2017)

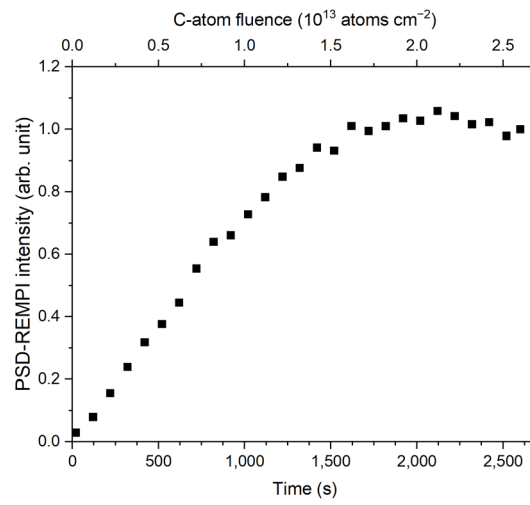


Supplementary Fig. 1 | Timing chart and scheme for the PSD-REMPI measurement.

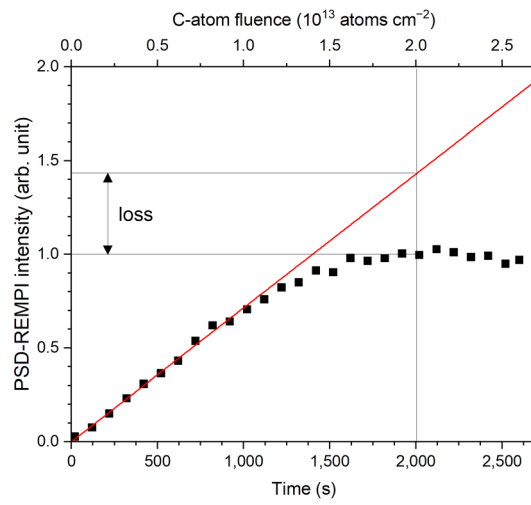
The timing chart is presented on the left side. The schemes for C atom deposition, photodesorption by a PSD laser, and ionization of C atom by the REMPI laser are shown in the right side. Because C atoms are deposited continuously, the PSD-REMPI C⁺ signal intensity increases as a function of time.



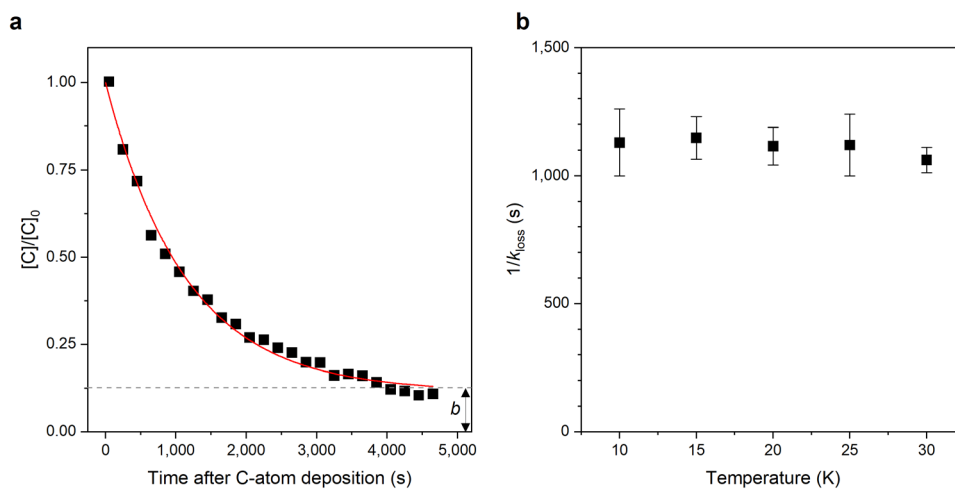
Supplementary Fig. 2 | PSD-REMPI spectrum of C atoms adsorbed on ASW. After photodesorption by the PSD laser (532 nm), the C atoms were ionized by the (2 + 1) REMPI scheme via the $2s^22p3p (^3D_{J'}) \leftarrow 2s^22p^2 (^3P_{J''})$ transition, where J' and J'' are the total angular momenta of intermediate and initial states, respectively. The assignments ($J' \leftarrow J''$) for the observed transitions are indicated.



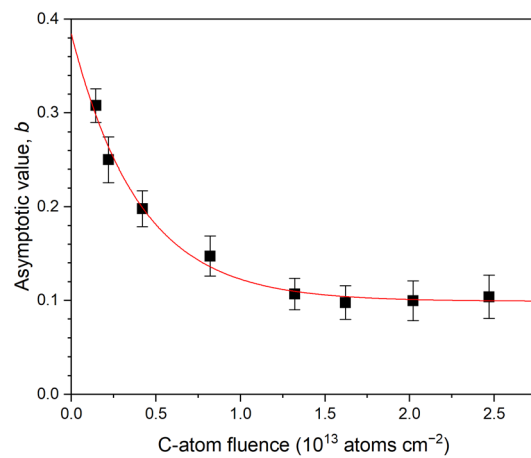
Supplementary Fig. 3 | PSD-REMPI intensities during C atom deposition. The PSD-REMPI measurements were performed during continuous C atom deposition on np-ASW at 10 K. The C atom deposition was started at $t = 0$ with a flux of 1×10^{10} atoms $\text{cm}^{-2} \text{s}^{-1}$. The total fluence is indicated on the top axis.



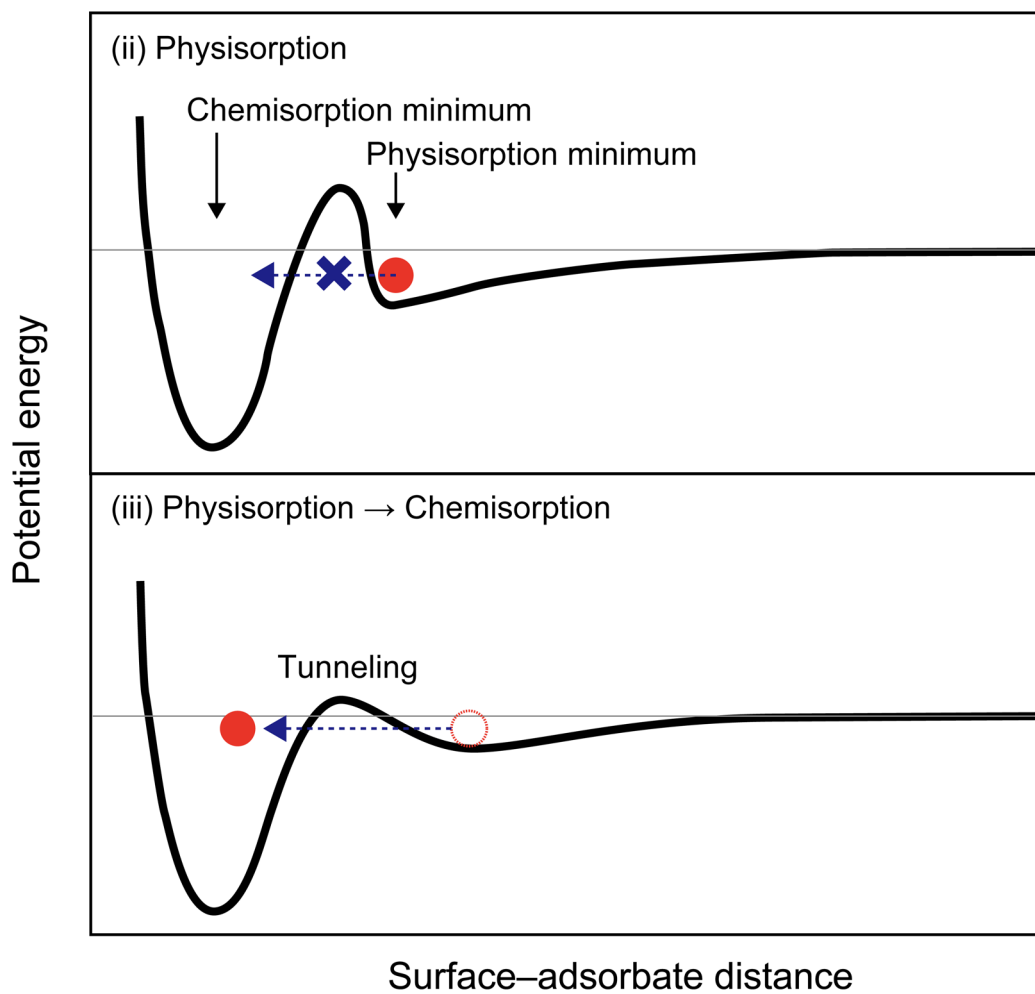
Supplementary Fig. 4 | Time evolution of PSD-REMPI intensities during C atom deposition. Experimental data are shown in black squares. The red line represents the fitting result assuming the linear relationship between PSD-REMPI intensity and C-atom fluence.



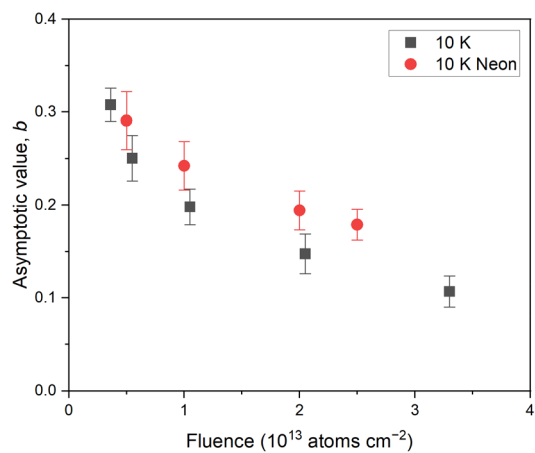
Supplementary Fig. 5 | Time evolution of PSD-REMPI intensities after terminating C atom deposition. (a) After terminating C atom deposition, PSD-REMPI measurements were performed with 100 s intervals, and the measured intensities are plotted by black squares. The presented data were obtained at 10 K. Red line is the result of fitting according to equation (S1). The same measurements were performed for temperatures at 15, 20, 25, and 30 K. (b) The decay time constants ($1/k_{\text{loss}}$) as a function of surface temperatures. Data are presented as $1/k_{\text{loss}} \pm \text{SD}$. The error bars represent the standard deviation (1-sigma) estimated in the least squares fitting of decay curves according to equation (S1).



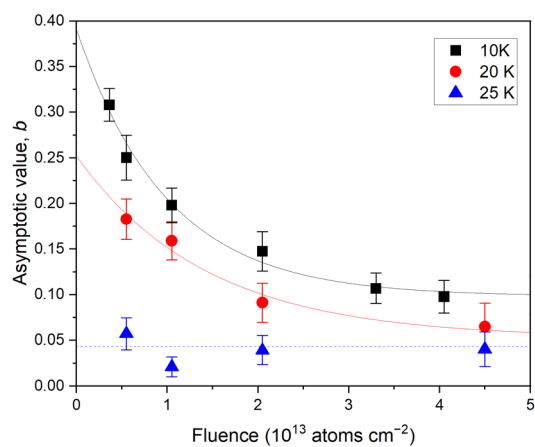
Supplementary Fig. 6 | Asymptotic values as a function of C-atom fluence. Asymptotic values (b in equation (S1)) are plotted as a function of C-atom fluence. Data are presented as $b \pm \text{SD}$. The error bars represent the standard deviation (1-sigma) estimated in the least squares fitting of decay curves according to equation (S1). Red line is the result of fitting with a single exponential function.



Supplementary Fig. 7 | Potential energy schemes for adsorption. The potential energy schemes for type ii and iii binding sites as a function of surface-adsorbate distance. Dashed arrows indicate the transformation path from physisorption to chemisorption via the quantum mechanical tunneling.



Supplementary Fig. 8 | Asymptotic values at different C-atom fluences. The asymptotic values, b , determined for various C-atom fluences. Black squares represent the results from a normal C-atom deposition and red circles represent those from co-deposition of C atoms and neon. Data are presented as $b \pm \text{SD}$. The error bars represent the standard deviation (1-sigma) estimated in the least squares fitting of decay curves according to equation (S1).



Supplementary Fig. 9 | Asymptotic values at temperatures 10–25 K. The asymptotic values, b , determined for various C-atom fluences and at temperatures 10 (black squares), 20 (red circles), and 25 K (blue triangles). Solid lines for 10 and 20 K are the result of single exponential fitting to extrapolate the experimental data to very low fluence. Data are presented as $b \pm \text{SD}$. The error bars represent the standard deviation (1-sigma) estimated in the least squares fitting of decay curves according to equation (S1).